Water Air Soil Pollut (2016) 227: 428
DOI 10.1007/s11270-016-3131-5

Impact of Stream Geomorphology on Greenhouse Gas Concentration in a New York Mountain Stream

Philippe Vidon · **Satish Serchan**

Received: 14 June 2016 / Accepted: 18 October 2016 / Published online: 3 November 2016

Abstract As increased greenhouse gas concentrations (GHG: N_2O, CO_2, CH_4) in our atmosphere remain a major concern, better quantifying GHG fluxes from natural systems is essential. In this study, we investigate GHG concentrations in saturated riparian sediments (dry, wet, mucky), streambed hyporheic zone sediments (pools, riffles), and stream water in a New York mountain stream for summer baseflow conditions, and attempt to identify the primary drivers (e.g., DO, DOC, NO_3^-, and NH_4^+, temp) of GHG concentrations at these locations. Although DO, DOC, NO_3^-, and NH_4^+ concentration patterns certainly explained some of the observed trends, the overall differences in GHG abundance in riparian water vs. hyporheic pool water vs. hyporheic riffle water strongly suggest that water velocity/mixing with the atmosphere is a key control on GHG concentration across locations. When all floodplain locations are considered, in-stream pools are hot spots of CO_2 and CH_4 concentrations relative to other in-stream locations. On the other hand, riparian areas are hot spots of CH_4 and CO_2 concentrations relative to stream locations. No clear patterns are observed for N_2O.

Keywords Dissolved gases · Concentration excess · Hyporheic zone · Groundwater · Stream

P. Vidon (✉) · S. Serchan
Department of Forest and Natural Resources Management, The State University of New York College of Environmental Science and Forestry (SUNY-ESF), Bray 320, 1 Forestry Drive, Syracuse, NY 13210, USA
e-mail: pgvidon@esf.edu

S. Serchan
e-mail: serchans@oregonstate.edu

S. Serchan
Water Resources Graduate Program, The Oregon State University (OSU), Corvallis, OR 97330, USA

S. Serchan
Corvallis Forestry Sciences Laboratory, United States Department of Agriculture, Pacific Northwest Research Station, 3200 SW Jefferson Way, Corvallis, OR 97331, USA

1 Introduction

As increased greenhouse gas concentrations (GHG: N_2O, CO_2, CH_4) in our atmosphere remain a major concern worldwide, better quantifying GHG fluxes from natural systems (e.g., streams, riparian zone soils, wetlands, etc.) is essential to fully comprehend the relative importance of anthropogenic vs. natural emissions at regulating GHG concentrations in our atmosphere (Butman et al. 2016; Stanley et al. 2016). In natural systems, aerobic respiration is the main mechanism responsible for CO_2 emission, while CH_4 is consumed by methane oxidation and produced via methanogenesis, or the reduction of organic matter with CO_2 as an electron acceptor under much reduced conditions (Hedin et al. 1998). Although N_2O is primarily produced via incomplete heterotrophic denitrification under anaerobic conditions, nitrification can also produce N_2O gas under aerobic conditions (Naiman et al. 2010). Like many heterotrophic processes, these

reactions (aerobic respiration, nitrification, methane oxidation, denitrification, methanogenesis) are mainly influenced by temperature, organic carbon availability (electron donor), soil moisture/water availability, and electron acceptor dynamics (O_2, NO_3^-, SO_4^{2-}, CO_2) (Hedin et al. 1998; Naiman et al. 2010; Vidon et al. 2010). Once produced, GHGs in natural systems can move either via direct efflux to the atmosphere via the soil-atmosphere interface, or as dissolved gases in water in streams, lakes, or interstitial water in riparian and wetland soils (Bowden and Bormann 1986; Clymo et al. 1995; Burgin and Groffman 2012). Nevertheless, although many studies document GHG emissions at the soil-atmosphere interface (Jacinthe and Lal 2004; Ullah and Moore 2011; Morse et al. 2012; Fisher et al. 2014), fewer directly quantify GHG concentration in stream or interstitial water in riparian and/or stream sediments. However, several recent studies show that transport of GHG to seeps and streams via soil water can be an important pathway for soil-derived GHG to reach the atmosphere-water interface (e.g., streams, seeps, lakes) (Bowden and Bormann 1986; Rothfuss and Conrad 1998; Burgin and Groffman 2012; Raymond et al. 2013). For instance, Bowden and Bormann (1986) showed that soil-derived N_2O fluxes transported to streams and seeps via soil water from a clear-cut watershed were two orders of magnitude over the atmospheric equilibrium. Elsewhere, Rothfuss and Conrad (1998) showed that interstitial water in poorly drained rice paddy soils was hypersaturated with dissolved CH_4 due to anoxic conditions. Similarly, soil-derived N_2O can be a significant component of stream N_2O budgets in agricultural watersheds (Mosier et al. 1998; Beaulieu et al. 2008; Werner et al. 2012). On a global scale, Beaulieu et al. (2011) estimated that streams could contribute approximately 10 % of worldwide N_2O emissions. Butman and Raymond (2011) also showed that fluxes of CO_2 from streams and rivers in the USA were sufficiently large to significantly affect estimates of global CO_2 fluxes in the environment.

In streams, understanding how much of each GHG (i.e., N_2O, CO_2, CH_4) is produced, and where "hot spots" or areas of disproportionally high GHG concentration occur is therefore essential to be able to better understand the role of streams and hyporheic zones in global emission of GHG by natural systems, and predict how various stream geomorphic features (e.g., pools, riffles, runs) may impact GHG concentrations in the water column and their release in the atmosphere (Stanley et al. 2016). For instance, pools, which are often associated with an accumulation of organic matter and low flow velocity within a stream channel, can be hot spots for CH_4 production due to low dissolved oxygen and organic carbon accumulation (Sanders et al. 2007). In contrast, well-oxygenated high flow velocity riffles can promote nitrification and the rapid transfer of GHG to the atmosphere (Beaulieu et al. 2011). In riparian zones, characterizing GHG concentration in soils and sediments is equally important owing to the strong connection that exists between streams and riparian sediments in many systems (Dent et al. 2001; McClain et al. 2003). In a broader watershed context, stream hyporheic zones and riparian zones are also potential hot spots of GHG production as the accumulation of organic matter, topography, mean residence time of reactants coupled with environmental factors such as hydrologic flowpaths, temperature, and soil moisture regimes all combine to enhance biogeochemical activities in these environments (McClain et al. 2003; Vidon et al. 2010). Understanding the dynamics of GHG concentrations in these systems and how concentration of GHG may vary from headwater to downstream locations is therefore also important (Stanley et al. 2016).

Within this context, forested mountain streams, where steep gradients and often well-developed pool-riffle sequences with well-developed hyporheic zones are often present, offer a unique opportunity to study the role of stream geomorphic features on GHG concentration in the subsurface, as well as the relative importance of biogeochemical variables (e.g., nitrate (NO_3^-), ammonium (NH_4^+), temperature (Temp), dissolved organic carbon (DOC), dissolved oxygen (DO)) at controlling N_2O, CO_2, and CH_4 concentration in both riparian and stream sediments from headwaters to downstream locations. In this study, we therefore investigate the concentration dynamics of N_2O, CO_2, and CH_4 in riparian sediments, streambed hyporheic sediments, and stream water in a New York mountain stream for summer baseflow conditions. We aim to (1) determine differences in GHG concentration between stream water and various types of riparian and streambed sediments from headwater to downstream locations and (2) determine the primary drivers (e.g., NO_3^-, NH_4^+, Temp, DOC, DO) of N_2O, CO_2, and CH_4 concentration. Fieldwork was conducted in July–August 2013 during baseflow conditions in Archer Creek in the Adirondack Mountains, New York, and based on multiple GHG

and water quality measurements at 35 riparian locations and 35 in-stream locations.

2 Materials and Methods

2.1 Site Description

Archer Creek is located in Archer Creek Watershed (515 m above sea level, 43° 59′ 32″ N, 74° 14′ 32″ W), a 135-ha forested catchment (1 % water, 6 % forested wetland, 93 % forest) located in the Adirondack Mountains, NY (Fig. 1). Climate is cool, moist, and continental. Between the years 1941 and 2007, the mean annual temperature was 5.0 °C, the mean annual precipitation was 1046 mm, and the mean annual snowfall was 303 cm (Mitchell et al. 2009). Precipitation in 2013 was 12 % greater than normal and was recorded at the National Atmospheric Deposition Program/National Trends Network Site (ID NY20) located in the Huntington Wildlife Forest approximately 2.0 km from the study stream. Surficial geology in the study watershed consists of glacial till composed of approximately 75 % sand and less than 10 % clay content (Christopher et al. 2006). Upland soils are sandy loam (Becket Mundal series) approximately 1 m thick with localized areas of deeper soil. Wetlands and valley-bottoms soils are generally Greenwood Mucky Peats deposits (hemic soil material) 1 to 5 m deep (Somers 1986). Archer Creek (11 % average slope) is composed of two upper branches, S14 and S15, with 16 and 10 % slope, respectively (Somers 1986).

2.2 Water Quality and Dissolved Gas Measurements

Two reaches (HW1 and HW2) were randomly selected in S15, two (HW3 and HW4) were randomly selected in S14, and three (LL1, LL2, and WL) were randomly selected in the lower reaches of Archer Creek (i.e., downstream of the S14–S15 confluence) (Fig. 1). Reaches HW1 and HW3 contain a high amount of mucky wet soils compared to HW2 and HW4 (Fig. 1). Although the LL2 reach was not directly influenced by a wetland like the WL reach, it was wetter (shallower water table) than the rockier LL1 reach higher up in the watershed (Fig. 1). Each selected reach was 20 m long and 12 m wide, with a 6-m line away from the centerline of the grid marking the outer extent of the study area for each reach for practical purposes. Within each reach, a total of 10 instrument clusters were installed: five in the riparian zone and five in the stream. Each instrument cluster consisted of a piezometer for water quality analysis and one silicone tube for GHG concentration measurements (see description below). Each in-stream cluster also had one extra silicone tube placed above the streambed for measuring GHG concentration in the stream water itself. In-stream instrument clusters (IS) were grouped in three categories: pools with fine textured (sandy loam) bed sediments (IS-Pool-Fine, $n = 3$), pools with coarse (sand) textured bed sediments (IS-Pool-Coarse, $n = 19$), and riffles or runs (Riffle or Run, $n = 13$). Riparian instrument clusters (RZ) were installed in three types of sites: moist sandy loam soil (RZ-Dry), mucky/wet soil (RZ-Mucky), and permanently saturated organic soil (RZ-Wet) based on soil organic matter content/texture and water table depth at the time of measurement (summer baseflow).

Piezometers consisted of 50 cm long 1.67 cm ID PVC pipe with 20 cm long slotted ends at the bottom and were installed at a depth of 40 cm below ground surface (BGS) using a screw auger in the riparian zone (RZ) and 20–30 cm BGS at IS locations. On four different dates during the July–August 2013 summer baseflow period, piezometers were purged and allowed to refill, and 140 mL of water was subsequently collected for analysis. Groundwater temperature and dissolved oxygen (DO) in piezometers were measured in the field using Hanna DO meters (Hanna HI9146, Hanna Instrument Inc. Smithfield, RI, USA) and Hanna Temp/ORP meters (Hanna HI9125, Hanna Instrument Inc. Smithfield, RI, USA). Water samples were collected with Tygon tubing using a three-way valve connected to a syringe to prevent contact with the atmosphere while pumping (Vidon and Hill 2004). DO was then measured with the DO meter by inserting the oxygen probe into the syringe (Vidon and Hill 2004). Water samples were then kept in a cooler and filtered using 0.7 μm GF/F filters (Whatman Inc., Florham Park, NJ) that same day. An aliquot of each filtered sample was then frozen until analysis (within 1 month) for nitrate (NO_3^-) and ammonium (NH_4^+) on a Bran + Luebbe Autoanalyzer 3 (SEAL Analytical, Mequon, WI, USA) using standard colorimetric methods (Clesceri et al. 1998). For DOC analysis, an aliquot of each filtered sample was acidified using 2 M H_2SO_4 and refrigerated until analysis for DOC using a Tekmar carbon analyzer (Phoenix8000, Tekmar, Mason, OH). For all analyses, triplicate

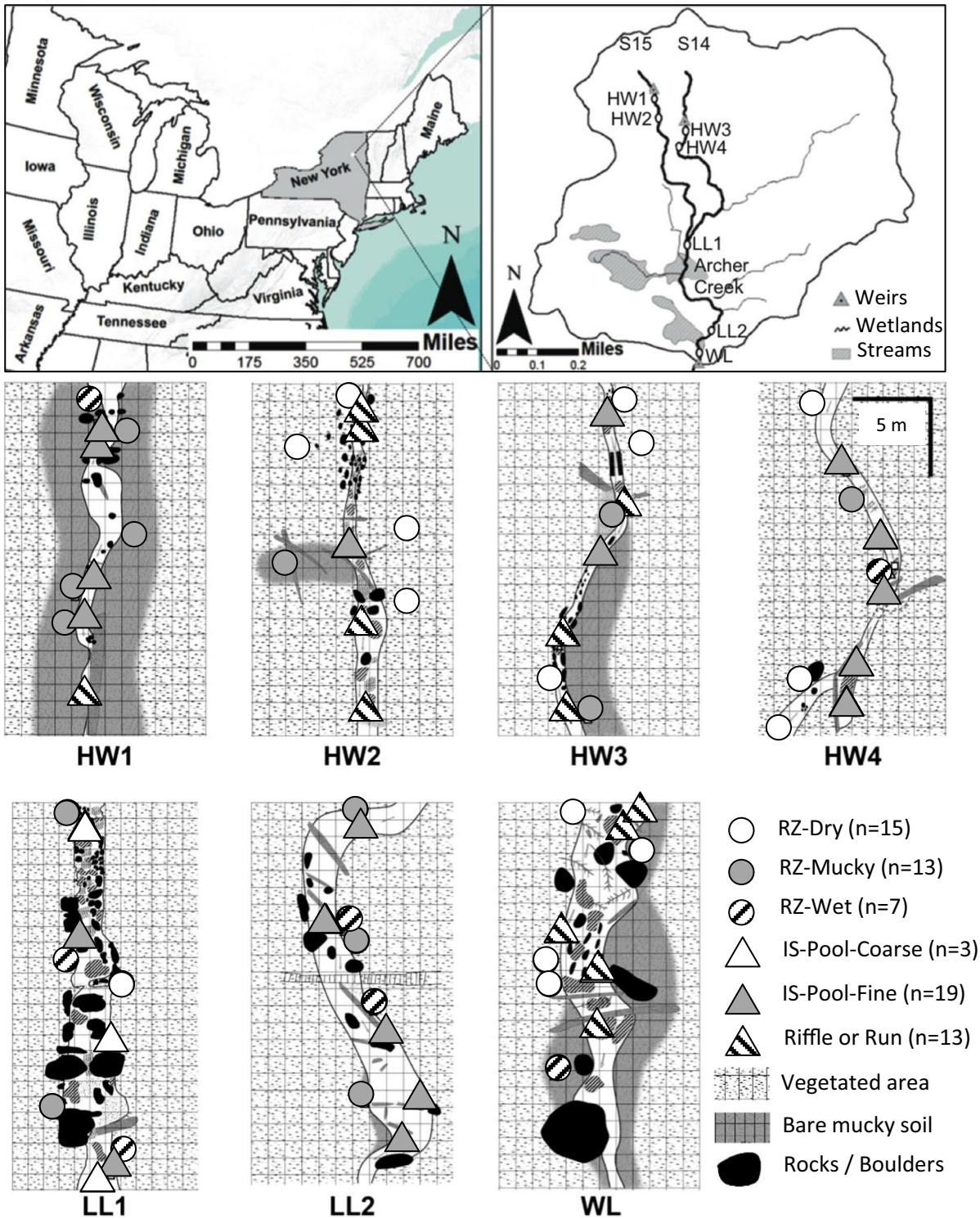

Fig. 1 Archer Creek watershed location in New York, USA (*upper left*), and locations of the seven stream reaches studied in Archer Creek watershed (*upper right*). Planar views of the seven stream reaches (bottom). *HW1–4* headwater locations 1 through 4, *LL1 and LL2* lowland locations 1 and 2, *WL* wetland location, *RZ-Dry* dry riparian zone sediments, *RZ-Mucky* mucky riparian zone sediments, *RZ-Wet* wet riparian zone sediments, *IS-Pool-Fine* in-stream sediment pool with fine textured sediments, *IS-Pool-Coarse* in-stream sediment pool with coarse textured sediments, *Riffle or Run* riffle or run

analyses were run on 10 % of the samples, and check-standards were analyzed for every 10 samples.

Silicone tubes for GHG concentration measurements were based on the design developed by Jacinthe and Groffman (2001) and based on the unique properties of silicone rubber (permeable to gases, impermeable to water). When submerged and inserted in piezometers either in the water column (stream water), in groundwater (RZ-Dry, RZ-Wet, RZ-Mucky), or hyporheic water (IS-Pool-Coarse, IS-Pool-Fine, Riffle or Run), the concentration of the gases in the silicone tube is dependent on the concentration of the gases in the water surrounding the silicone tube (see calculation below; Jacinthe and Groffman 2001). Each silicone tube consisted of a 15-cm-long section of silicone tube (Versilic Silicone tubing, 0.5 in. I.D., 11/16 in. O.D.) sealed with rubber stoppers and silicone gel sealant, and connected to the water surface via a 30-cm-long section of Tygon tubing (1/8 in. I.D., ¼ in. O.D.) connected to a two-way valve. Whenever water samples were collected on four dates in summer 2013, silicone tubes were inserted in the piezometers (after water samples were collected) and left to equilibrate overnight. By plugging the top of the piezometers and filling-in the area immediately above the silicone tubes with foam material, we ensured that all the silicone tubes inserted in the piezometers were isolated from ambient conditions in the atmosphere above the streambed. When sampling the silicone tubes, the two-way valve connected to the silicone tube via the Tygon tubing was connected to a syringe and 15 mL of gases in the collapsible silicone tube was collected and immediately transferred to pre-evacuated gas chromatograph vials. Samples were kept out of the light during transport and storage periods and were usually analyzed within 2 weeks of collection. Carbon dioxide, CH_4, and N_2O concentrations were analyzed utilizing a Shimadzu GC-2014® gas chromatograph (Shimadzu Corporation, Kyoto, Japan) equipped with a flame ionizing detector and an electron capture detector interfaced with a CombiPal® autosampler (LEAP Technologies, Carrboro, NC). The stationary phase consisted of a Porapak Q® precolumn (90 cm long) and Hayesep D® analytical columns (180 cm long). The GC was calibrated using standard gases obtained from Alltech (Deerfield, IL). To prevent moisture buildup in the GC columns, the GC oven was heated (150 °C) for 15 min for every 20 samples.

The concentration of each of the dissolved gases (CO_2, CH_4, N_2O) in the water was calculated based on the concentration of each gas in the silicone tube based on Henry's law:

$$[X]_{aq} = \left([X]_g M_w\right) / \left(HRT \times 10^6\right) \quad (1)$$

where $[X]_{aq}$ is the concentration of gaseous species X in solution (mg L^{-1} water), $[X]_g$ is the concentration of species X in the gas phase (μL L^{-1} air, *v*/*v*), M_w is the molar relationship (mg X mol^{-1}), H is the dimensionless constant ($H = 0.8$, 23.3, and 1.1 for CO_2, CH_4, and N_2O, respectively), R is the universal gas constant (8.205×10^{-2} l atm K^{-1} mol^{-1}), and T is the temperature (°K). Subsequently, we calculated the degree of saturation of the water for each gas ($xsCO_2$, $xsCH_4$, xsN_2O) as the excess gas above or below atmospheric equilibrium ($xsC_{gas} = 0$ at equilibrium, <0 if undersaturated, > 0 if oversaturated) as:

$$xsC_{gas} = C_{obs} - C_{sat} \quad (2)$$

where C_{gas} is a gas species (CO_2, CH_4, or N_2O), C_{obs} is the dissolved concentration of that gas from Formula 1 ($[X]_{aq}$) expressed as a molar concentration (i.e., μmol/L as opposed to mg/L) and C_{sat} is the theoretical equilibrium concentration of that gas in water based on water temperature and the known concentration of that gas in the atmosphere. In Eq. 2, C_{sat} at a given temperature is calculated using Henry's law:

$$p = k_H \times C_{sat} \quad (3)$$

where p is the partial pressure of the gas in the atmosphere, k_H is Henry's law volatility constant, and C_{sat} is the aqueous phase molar concentration of the species. In Eq. 3, k_H or $k_H(T)$ for any given temperature (T) is determined using a form of Van't Hoff equation

$$k_H(T) = k_H(T^\circ)\mathrm{e}\left[-C\left(\frac{1}{T} - \frac{1}{T^\circ}\right)\right] \quad (4)$$

where k_H (T^o) for CO_2 is 29.4, 0.048 for N_2O, and 0.458 for CH_4. In this equation, T^o is 298 K and the constant C value for CO_2 is 2400, 2675 for N_2O, and 1750 for CH_4.

2.3 Data Analysis

At each location, data from all four dates were averaged before analysis to account for temporal variability between summer baseflow sampling dates. A one-way analysis of variance (ANOVA) was used to analyze the data (Factor = RZ-DRY, RZ-Mucky, etc.). Following a significant statistical effect, post hoc pairwise differences were analyzed using Tukey's multiple comparison tests. To meet the assumption of normality prior to parametric statistical analyses, most data were log transformed and normality determined using an Anderson–Darling test. Linear correlations between each GHG species and all predictor variables (DOC, DO, NO_3^-, NH_4^+, and temperatures) were quantified using Pearson correlation coefficients. Statistical analyses were performed using SAS 9.4/9.3 (SAS Institute Inc., Cary, NC, USA), and boxplots and graphs were generated in Minitab 16 (Minitab Inc., State College, PA, USA) and Microsoft Excel 2010 (Microsoft Corporation, Redmond, CA, USA).

3 Results

3.1 Water Quality Measurements

Mean DO concentrations in the various stream hyporheic zone locations (IS-Pool-Fine, IS-Pool-Coarse, Riffle or Run) and riparian zone groupings (RZ-Dry, RZ-Wet, RZ-Mucky) ranged from 7.0 mg/L (Riffles) to 3.0 mg/L (RZ-Mucky), with lower values in the RZ-Mucky and RZ-Wet locations than at most other locations (Fig. 2). Significant differences between groups are shown on Fig. 2. DO in the stream water (11.0 mg/L) was significantly higher than in all other locations. With respect to DOC, mean DOC concentrations were generally higher at the RZ-Mucky and RZ-Wet sites (7.3–9.0 mg/L) and lower in the Riffle (2.9 mg/L) and in stream water (3.8 mg/L).

Mean NO_3^- concentrations varied between below detection limit (BDL; 0.01 mg/L) at the RZ-Wet sites to 0.4 mg/L in stream water, with only a few significant differences between groups (Fig. 2). Conversely, NH_4^+ was the highest at the RZ-Wet sites (0.4 mg/L) and lowest in stream water (BDL). For the four sampling dates, riparian groundwater temperatures (RZ-Wet, RZ-Dry, RZ-Mucky) and in-stream groundwater temperatures (IS-Pool-Fine, IS-Pool-Coarse, Riffle or Run) were generally not significantly different and remained in the 17.2–16.3 °C range. Stream water itself was however significantly cooler (13.7 °C).

3.2 Greenhouse Gas Concentration Measurements

Mean concentration of CO_2 in water ranged from 88.3 μmol/L in stream water to 362.4 μmol/L for sites in the RZ-Mucky group, with the highest values in the RZ-Wet and RZ-Mucky sites and lowest values in Riffle and Run sites and in stream water (Fig. 3). When expressed in terms of concentration in excess of saturation (i.e., the theoretical concentration based on atmospheric CO_2 concentration), the RZ-Mucky and RZ-Wet sites presented dissolved CO_2 concentration approximately 21 times in excess of atmospheric equilibrium, or in excess by approximately 344–345 μmol/L (Table 1). Among in-stream features, the degree of hyper CO_2 saturation ranged from 6 times (88.2 μmol/L) in riffles and runs to 12 times (192.0 μmol/L) in pools with fine textured sediments (IS-Pool-Fine).

Dissolved CH_4 study period average values were more variable than CO_2 and spanned two orders of magnitude. Some of the highest means for dissolved CH_4 occurred at RZ-Mucky sites (9.02 μmol/L), followed by RZ-Wet sites (4.46 μmol/L), whereas Riffle and Run sites (0.069 μmol/L) and RZ-Dry sites (0.78 μmol/L) had the lowest study period averages (Fig. 3). When expressed in term of saturation excess, all locations were oversaturated in CH_4, with saturation excess as high as 9.01 μmol/L or 1917 times above equilibrium at the RZ-Mucky sites, and lowest values in riffles and runs sites, with dissolved CH_4 concentrations only 0.012 μmol/L in excess of equilibrium or 14 times above equilibrium.

Unlike for CO_2 and CH_4, some of the highest dissolved N_2O concentrations were observed at RZ-Dry sites (mean = 0.034 μmol/L), while some of the lowest values were observed at RZ-Wet sites (mean = 0.012 μmol/L). IS locations generally presented intermediate dissolved N_2O concentrations (range of means = 0.016–0.020 μmol/L). Although oversaturated in N_2O (typically by 0.004–0.012 μmol/L except for the RZ-Dry sites where excess concentrations reached 0.026 μmol/L), both RZ and IS locations were only moderately oversaturated in N_2O (1.7 to 4.5 above equilibrium) compared to the levels of oversaturation observed for CH_4 or CO_2 (Table 1).

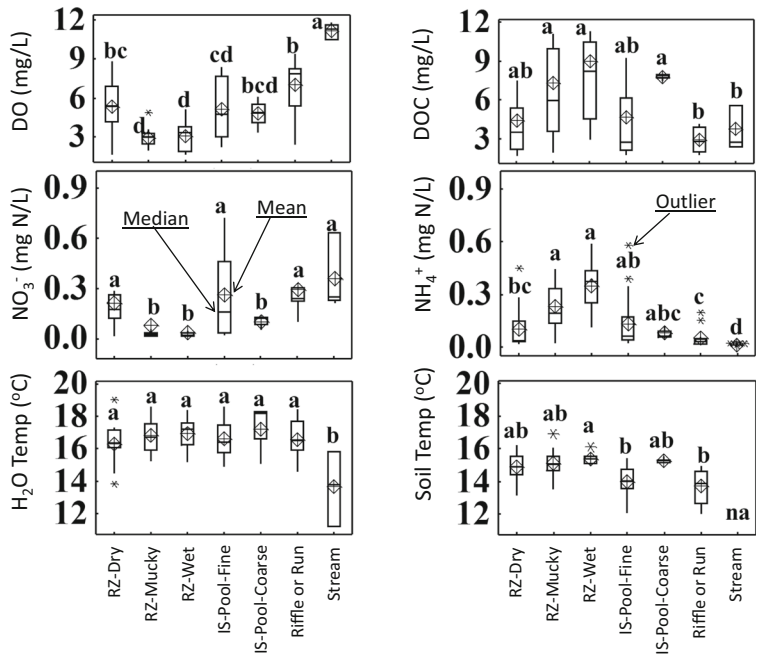

Fig. 2 Box plots (mean, median, 25th and 75th quartiles, and outliers) illustrating dissolved oxygen (*DO*), dissolved organic carbon (*DOC*), nitrate (NO_3^-), ammonium (NH_4^+), water temperature (H_2O *Temp*), and soil/sediment temperature (*Soil Temp*) for stream water (if applicable) and in hyporheic water/groundwater in each of the geomorphic features studied here across all seven stream reaches over the study period. *Letters a*, *b*, *c*, and *d* indicate differences between groups (see data analysis section for methods description). *RZ-Dry* dry riparian zone sediments, *RZ-Mucky* mucky riparian zone sediments, *RZ-Wet* wet riparian zone sediments, *IS-Pool-Fine* in-stream sediment pool with fine textured sediments, *IS-Pool-Coarse* in-stream sediment pool with coarse textured sediments, *Riffle or Run* riffle or run

When compared based on locations from headwaters (HW1–4) to downstream locations (LL1–2, WL), CH_4 concentrations are on average 4 times higher at downstream locations (5.8 μmol/L) than at upstream locations (1.5 μmol/L) (Table 2). Similarly, CO_2 concentrations are 1.5 times higher at downstream locations (303 μmol/L) than at upstream locations (199 μmol/L). However, the opposite is observed for N_2O with N_2O concentration twice as large at upstream locations (0.026 μmol/L) than at downstream locations (0.014 μmol/L). When expressed in terms of saturation excess, a similar pattern is observed (Table 2).

3.3 Correlation Analysis

Pearson correlation coefficients between mean concentration of CO_2, CH_4, and N_2O at each location over the four sampling dates and mean DOC, DO, NO_3^-, NH_4^+, and water temperature are shown in Fig. 4. When all the data are combined (i.e., RZ sites, IS sites), the concentration of CO_2 is most significantly ($p < 0.05$) correlated to DO ($r = -0.56$), NO_3^- ($r = 0.51$), and NH_4^+ ($r = 0.46$). On a site-by-site basis, other significant correlations (see Fig. 4 caption for p values) between CO_2 and individual variables occur but are not observed across the board in all locations.

For CH_4, although DO, temp, NO_3^-, NH_4^+, and DOC are significantly correlated to CH_4 (see Fig. 4 caption for p values), correlation coefficients remain low ($r = < \pm 0.3$). On a site-by-site basis, significant correlations with high r values are observed like at the RZ-Dry sites where CH_4 is moderately (and significantly) correlated to NH_4^+ ($r = 0.51$), or in Riffle and Run sites where CH_4 is moderately significantly correlated to DO ($r = -0.48$). However, high correlation coefficients (even if they are significant) do not occur consistently across all sites.

A similar pattern is observed for N_2O, with significant (when $r > 0.12$) but weak correlation ($r < 0.4$) between N_2O and mean DOC, DO, NO_3^-, NH_4^+, and water temperature when all the sites are combined. On a site-by-site basis, strong correlations exist such as at the RZ-Mucky sites where N_2O is strongly and significantly correlated

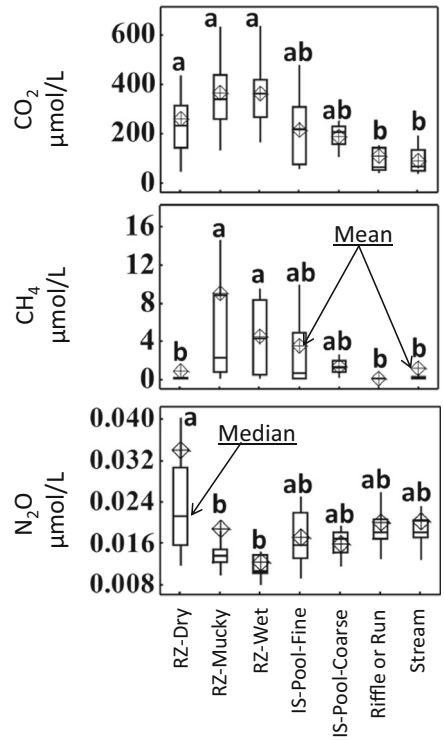

Fig. 3 Box plots (mean, median, 25th and 75th quartiles, and outliers) illustrating dissolved CO_2, N_2O, and CH_4 concentrations in stream water and in hyporheic water/groundwater in each of the geomorphic features studied here across all seven stream reaches over the study period. *RZ-Dry* dry riparian zone sediments, *RZ-Mucky* mucky riparian zone sediments, *RZ-Wet* wet riparian zone sediments, *IS-Pool-Fine* in-stream sediment pool with fine textured sediments, *IS-Pool-Coarse* in-stream sediment pool with coarse textured sediments, *Riffle or Run* riffle or run

to NO_3^- ($r = 0.63$), but this only occurs occasionally (Fig. 4).

4 Discussion

In this study, we reported both concentration and excess concentration (or concentration in excess of saturation) for each GHG (i.e., CO_2, CH_4, N_2O). Although variables depend on location (see Table 1), results are overall consistent with those found in the literature (Hope et al. 2001; Beaulieu et al. 2011; Werner et al. 2012; Stanley et al. 2016). For instance, in their investigation of spatial and seasonal variations in CO_2 and CH_4 concentrations in streams and adjacent soils at various sites located in a headwater stream draining a peatland catchment in upland Britain, Hope et al. (2001) reported values of dissolved CO_2 ranging from 3.57 to 7.5 mg/L (or 81–170 µmol/L) and dissolved CH_4 ranging from 0.04 to 34.6 mg/L (or 2–2157 µmol/L) across the studied sites for the summer period. Billett and Moore (2008) reported dissolved CO_2 concentration values ranging from 47.7 to 177 µmol/L and dissolved CH_4 concentration values ranging from 0.6 to 10 µmol/L during spring and autumn 2005 in surface waters draining the Mer Bleue peatland (Ontario, Canada). In Southern Ontario, Canada, Rosamond et al. (2012) reported dissolved N_2O concentrations ranging from 0.002 to 0.56 µmol/L in rivers. Elsewhere, Jacinthe et al. (2012) reported average CO_2 concentration of 58 µmol/L and CH_4 concentration of 0.6 µmol/L in streams draining a predominantly agricultural watershed located in Indiana, USA. Similarly, Werner et al. (2012) reported dissolved CO_2 concentrations (range 12.6 to 222 µmol/L), dissolved CH_4 concentrations (range 0.02 to 0.26 µmol/L), and dissolved N_2O

Table 1 Arithmetic mean (±standard deviation) of the concentration of each gas in micromoles per liter (CH_4, CO_2, N_2O) and of the degree of saturation in micromoles per liter ($xsCH_4$, $xsCO_2$, xsN_2O) and expressed as the ratio of the observed concentration (C_{obs}) and the theoretical equilibrium concentration of each gas based on temperature and concentration of each gas in our atmosphere (C_{sat}) for methane (CH_4), carbon dioxide (CO_2), and nitrous oxide (N_2O) in piezometers at riparian ($n = 35$) and in-stream ($n = 35$) locations over the study period (4 sampling dates). Actual concentrations (μmol/L) are shown in Fig. 3

Sites	CO_2 (μmol/L)	CH_4 (μmol/L)	N_2O (μmol/L)	$xsCO_2$	$xsCH_4$	xsN_2O	CO_2—C_{obs}/C_{sat}	CH_4—C_{obs}/C_{sat}	N_2O—C_{obs}/C_{sat}
RZ-Dry	258.7 ± 197.8	0.78 ± 3.0	0.034 ± 0.050	240.9 ± 198.0	0.78 ± 3.00	0.026 ± 0.050	14.8 ± 11.6	166 ± 642	4.5 ± 6.4
RZ-Mucky	362.4 ± 233.5	9.02 ± 19.89	0.019 ± 0.030	344.8 ± 234.6	9.01 ± 19.89	0.011 ± 0.030	20.8 ± 13.6	1917 ± 4240	2.5 ± 3.7
RZ-Wet	361.1 ± 257.8	4.46 ± 5.38	0.012 ± 0.005	343.6 ± 257.7	4.46 ± 5.39	0.004 ± 0.006	20.7 ± 14.1	967 ± 1191	1.7 ± 1.1
IS-Pool-Coarse	185.3 ± 94.44	1.35 ± 1.63	0.016 ± 0.008	167.8 ± 94.1	1.35 ± 1.63	0.008 ± 0.008	10.5 ± 5.0	286 ± 341	2.1 ± 1.0
IS-Pool-Fine	210.3 ± 159.9	3.52 ± 8.77	0.017 ± 0.009	192.0 ± 160.1	3.52 ± 8.77	0.009 ± 0.009	11.7 ± 9.0	734 ± 1796	2.2 ± 1.2
Riffle or Run	106.6 ± 122.4	0.07 ± 0.17	0.020 ± 0.013	88.2 ± 122.4	0.06 ± 0.17	0.012 ± 0.013	5.8 ± 6.7	14.2 ± 34.1	2.6 ± 1.5
Stream Water	88.3 ± 67.97	1.16 ± 8.39	0.020 ± 0.016	69.7 ± 68.1	1.16 ± 8.39	0.012 ± 0.015	4.8 ± 3.7	244 ± 1766	2.6 ± 1.7

RZ-Dry dry riparian zone sediments ($n = 60$), *RZ-Mucky* mucky riparian zone sediments ($n = 52$), *RZ-Wet* wet riparian zone sediments ($n = 28$), *IS-Pool-Fine* in-stream sediment pool with fine textured sediments ($n = 76$); *IS-Pool-Coarse* in-stream sediment pool with coarse textured sediments ($n = 12$), riffle or run ($n = 52$), stream ($n = 140$)

Table 2 Arithmetic mean (±standard deviation) of the concentration of each gas in micromoles per liter (CH_4, CO_2, N_2O) and of the degree of saturation in micromoles per liter ($xsCH_4$, $xsCO_2$, xsN_2O) and expressed as the ratio of the observed concentration (C_{obs}) and the theoretical equilibrium concentration of each gas based on temperature and concentration of each gas in our atmosphere (C_{sat}) for methane (CH_4), carbon dioxide (CO_2), and nitrous oxide (N_2O) in piezometers for stream reaches HW1–4, LL1–2, and WL over the study period (see Fig. 1 for acronym definitions)

Sites	CO_2 (μmol/L)	CH_4 (μmol/L)	N_2O (μmol/L)	$xsCO_2$	$xsCH_4$	xsN_2O	CO_2—C_{obs}/C_{sat}	CH_4—C_{obs}/C_{sat}	N_2O—C_{obs}/C_{sat}
HW1	176.7 ± 120.8	0.75 ± 2.09	0.020 ± 0.008	158.4 ± 121.2	0.75 ± 2.09	0.012 ± 0.008	9.8 ± 7.0	157 ± 432	2.7 ± 1.3
HW2	130.4 ± 105.1	0.10 ± 0.26	0.019 ± 0.011	112.3 ± 105.3	0.09 ± 0.26	0.011 ± 0.011	7.3 ± 6.0	20 ± 54	2.5 ± 1.6
HW3	289.4 ± 262.8	4.77 ± 17.33	0.019 ± 0.016	271.0 ± 263.4	4.76 ± 5.02	0.011 ± 0.015	16.3 ± 15.4	1031 ± 3792	2.4 ± 1.7
HW4	201.4 ± 212.1	0.16 ± 0.56	0.047 ± 0.066	183.6 ± 212.5	0.15 ± 0.56	0.039 ± 0.066	11.7 ± 12.6	32 ± 113	6.2 ± 8.2
LL1	271.9 ± 134.6	4.10 ± 5.02	0.014 ± 0.006	254.4 ± 134.5	4.09 ± 5.02	0.006 ± 0.006	15.6 ± 7.8	877 ± 1086	1.9 ± 0.8
LL2	426.6 ± 211.3	12.49 ± 17.50	0.011 ± 0.005	408.8 ± 211.3	12.49 ± 17.50	0.003 ± 0.006	24.2 ± 11.7	2624 ± 3585	1.6 ± 0.9
WL	209.3 ±211.1	0.85 ± 3.14	0.016 ± 0.008	191.6 ± 210.9	0.81 ± 3.14	0.008 ± 0.008	11.7 ± 11.5	178 ± 667	2.2 ± 1.1

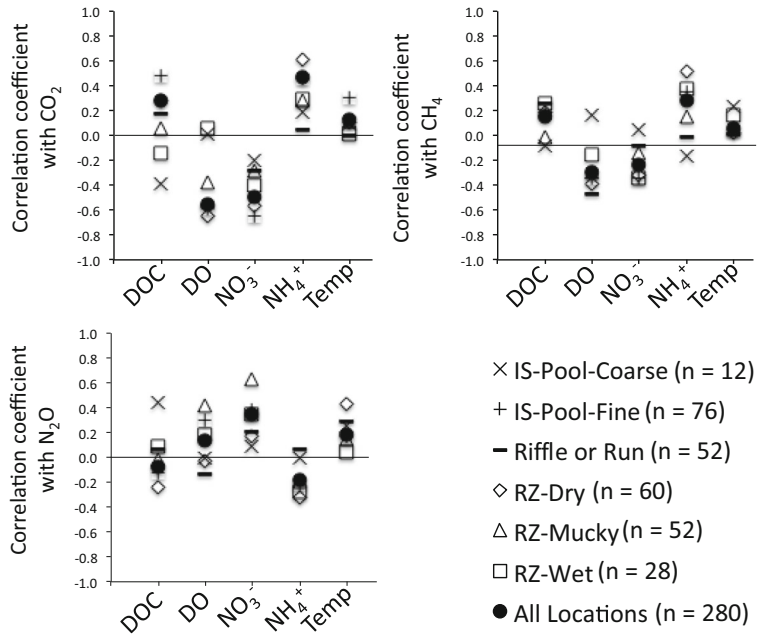

Fig. 4 Correlation coefficient between dissolved CO_2, N_2O, and CH_4 concentrations and select water quality parameters across all locations over the study period. Dissolved organic carbon (*DOC*), dissolved oxygen (*DO*), nitrate (NO_3^-), ammonium (NH_4^+), *Temp* water temperature, *RZ-Dry* dry riparian zone sediments ($n = 60$, $p < 0.05$ if $|r| > 0.25$), *RZ-Mucky* mucky riparian zone sediments ($n = 52$, $p < 0.05$ if $|r| > 0.27$), *RZ-Wet* wet riparian zone sediments ($n = 28$, $p < 0.05$ if $|r| > 0.37$), *IS-Pool-Fine* in-stream sediment pool with fine textured sediments ($n = 76$, $p < 0.05$ if $|r| > 0.23$), *IS-Pool-Coarse* in-stream sediment pool with coarse textured sediments ($n = 12$, $p < 0.05$ if $|r| > 0.54$), Riffle or Run ($n = 52$, $p < 0.05$ if $|r| > 0.27$), all locations ($n = 280$, $p < 0.05$ if $|r| > 0.12$)

concentrations (range <0.01 to 0.7 μmol/L) across several small baseflow-dominated stream ecosystems in central Wisconsin, USA, consistent with our findings.

When concentrations (and associated concentration excess) of each GHG are compared between geomorphic features (Table 1), it appears that differences in concentration are primarily driven by advective/dispersion processes, and this in spite of clear relationships between specific GHG and key predictive variables (NO_3^-, NH_4^+, DO, etc.; Fig. 4). Indeed, although no clear patterns are observed for N_2O, data clearly show that in fast moving riffles where enhanced hyporheic flow likely occurs (Kasahara and Hill 2005), CO_2 and CH_4 concentrations in the hyporheic zone (where samples were collected) are much lower than in slow moving pool hyporheic water, at least for summer baseflow conditions when observations were made. Similarly, CO_2 and CH_4 concentrations in riparian water are generally higher than in hyporheic water, especially in the mucky (RZ-Mucky) and wet (RZ-Wet) areas of the riparian zone where close to saturated conditions likely hinder GHG diffusion to the atmosphere. Further, similar dissolved GHG concentrations in stream water as in hyporheic riffle water are consistent with losses to the atmosphere at these locations. The lower GHG concentrations in stream water and hyporheic riffle water than in pool hyporheic water or riparian water are also consistent with longer residence times in riparian and pool hyporheic water and lower mixing rates with stream water at these locations.

Of course, the strong relationships between GHG concentration and water velocity (i.e., RZ vs. pool vs. riffle) do not mean that the underlying biogeochemical processes do not differ between geomorphic features, and that the gross production of gases across geomorphic features does not vary. Indeed, riparian water samples generally contain greater DOC concentrations than hyporheic water samples or stream water (Fig. 2) and are associated with higher CH_4 concentrations than at other locations. This is especially clear at the RZ-Mucky and RZ-Wet sites where high soil organic carbon (electron donor for methanogenesis) is likely to be higher than at other locations due to the presence of black organic soil at these locations. These locations (RZ-Wet and RZ-Mucky) also harbor lower DO and higher NH_4^+ concentrations than other locations, which is consistent with anoxic conditions limiting nitrification (strictly aerobic

process) and leading to NH_4^+ accumulation, and higher rates of methanogenesis at these locations than others (Hefting et al. 2003; Naiman et al. 2010).

Interestingly, these wet organic-rich locations where higher CH_4 concentrations were observed in the riparian zone also present high dissolved CO_2 concentration (Fig. 3). Although higher soil organic carbon content at the RZ-Wet and RZ-Mucky sites than at others could in theory boost aerobic respiration and associated CO_2 emissions, higher CH_4 concentrations, lower DO, and higher NH_4^+ (indicative of NH_4^+ accumulation owing to nitrification inhibition under low oxygen availability conditions) suggest that enhanced aerobic respiration is unlikely to be the main process responsible for higher CO_2 production at these locations. Instead, some studies have noted the association between CH_4 and CO_2 production under low oxygen conditions due to methanogenesis via acetate fermentation in peatland catchments with soil likely similar to those found in the RZ-Mucky and RZ-Wet areas (Hope et al. 2001). Another possible explanation could be the result of denitrification actively occurring at these sites (consistent with the low NO_3^- at these locations; Fig. 2) because CO_2 can also be a byproduct of heterotrophic denitrification (Hedin et al. 1998). Overall, the association of high dissolved CO_2 with low DO locations is also consistent with the previously mentioned negative correlation between CO_2 and DO when all the sites are combined (Fig. 4).

Beyond the underlying biogeochemical processes, when GHG concentrations are analyzed based on location (i.e., headwaters vs. downstream locations), downstream locations harbor significantly ($p < 0.05$) higher CH_4 and CO_2 concentrations than upstream locations and vice versa for N_2O (Table 2). Although informative from a management standpoint, these differences are a direct function of the distribution of key geomorphic features between locations. For instance, CH_4 concentrations are the highest in the LL2 reach (Table 2) where features with high CH_4 concentrations (RZ-Mucky, RZ-Wet, IS-Pool-Fine; Fig. 3) dominate (Fig. 1). Similarly, N_2O concentrations are higher at headwater locations (Table 2) because most RZ-Dry locations (11 out of 15) where high N_2O concentrations are observed (Fig. 3) are located in HW1–4 (Fig. 1). Therefore, although differences in GHG concentration are observed as a function of location (i.e., headwater vs. downstream), data suggest that these differences are simply a function of the relative importance of key geomorphic features among reaches. This indicates that overall, understanding the distribution of stream geomorphic features is essential to understand spatial differences in GHG concentration in streams and associated riparian zones, and this more so than simply classifying stream reaches based on their headwater or downstream location.

Aside from the impact of geomorphological aspects on GHG concentrations, when correlation coefficients between individual GHGs and water quality parameters are investigated, overall CO_2 is negatively correlated to NO_3^- because of the higher CO_2 concentration and lower NO_3^- concentrations observed at the RZ-Mucky and RZ-Wet sites relative to other locations (pool, riffle, stream water). For the same reasons (i.e., contrast between RZ-Mucky/RZ-Wet and other locations), CO_2 is also positively correlated to DOC and NH_4^+. With respect to CH_4, data indicate a positive correlation between CH_4 and temperature, which is consistent with methanogenesis being temperature sensitive (Van Hulzen et al. 1999). For N_2O, while a positive correlation between N_2O and NO_3^- is consistent with N_2O production being influenced by the presence of NO_3^-, this correlation alone sheds little light on the underlying processes driving N_2O concentration as NO_3^- can influence both nitrification and denitrification and that both of these processes can produce N_2O (Hedin et al. 1998; Naiman et al. 2010).

Ultimately, it is likely that a combination of production and diffusion controls GHG concentrations in hyporheic water for summer baseflow conditions. Indeed, although DO, DOC, NO_3^-, and NH_4^+ concentration patterns certainly explain some of the observed trends (see above), the overall differences in GHG excess (Table 1) in RZ water vs. hyporheic pool water vs. hyporheic riffle water strongly suggest that water velocity/mixing with the atmosphere in sections of the stream with enhanced hyporheic exchange such as riffle sections (Kasahara and Hill 2005) vs. pool section or riparian water also strongly impacted GHG concentrations across the study reaches. Although some GHGs are certainly exported as dissolved gases in stream water (Mosier et al. 1998; Beaulieu et al. 2008; Butman and Raymond 2011; Werner et al. 2012), the generally lower levels of excess saturation in stream water than at most locations (especially for CO_2 and CH_4; Table 1) suggest that much of the gases entering the stream water column through hyporheic exchange quickly evade to the atmosphere. As seen in other studies (e.g., Werner et al. 2012), constant GHG production in stream sediments

(as indicated by excess concentration) nevertheless prevents the stream from reaching equilibrium with the atmosphere, which is consistent with other works showing that streams likely play an important role in terms of GHG export at the watershed scale both through evasion to the atmosphere and transport to downstream locations (Beaulieu et al. 2008; Butman and Raymond 2011).

When all floodplain locations are considered, no clear differences in N_2O concentrations are consistently observed between geomorphic features, except at the RZ-Dry sites where N_2O concentrations tend to be consistently higher than at other locations. However, in-stream pools are hot spots of CO_2 and CH_4 concentrations relative to other riffle or run locations, and RZ-Wet and RZ-Mucky areas are hot spots of CH_4 and CO_2 concentrations relative to IS locations, at least for summer baseflow conditions when the study was conducted. In this context, it is however important to note that pools only represent a fraction (about 25 %) of stream features in the watershed and that RZ-Wet and RZ-Mucky areas are limited to small areas along the stream where mucky soils are present or to wetland areas (5.7 % of total area in the watershed; Gomez et al. 2016). This suggests that on an areal basis, other areas of the watershed (i.e., pools and runs, hillslopes) may produce a larger amount of GHG (Gomez et al. 2016). The relative importance of each of these areas may also change based on the time of year as temperature, moisture, and nutrient availability change with seasons (Gomez et al. 2016).

However, in spite of its limitations, this initial study of concentrations and concentration excess (by definition due to GHG production) of GHG in floodplain waters for summer baseflow conditions provides unprecedented insights into the distributions of dissolved CO_2, CH_4, and N_2O gases in stream, hyporheic, and riparian water, and the potential role of streams at transporting dissolved gases downstream and at releasing gases to the atmosphere, at least for summer baseflow conditions. However, more studies should be conducted to capture GHG dynamics at these locations over longer periods of time (seasons, years) and a range of flow conditions (spring baseflow, snowmelt period, etc.) to fully comprehend the relative importance of riparian vs. in-stream locations at controlling GHG concentrations at the reach scale on an annual basis (along with underlying biogeochemical processes), so solid stream annual GHG budgets can be developed for the entire stream length and applied to other forested watersheds.

Acknowledgments This project was supported by a US Geological Survey 104B grant (Award# 61103-10081) to P. Vidon through the New York Water Resources Institute in partnership with the New York Department of Environmental Conservation—Hudson River Estuary Program. Satish Serchan was supported though the US Department of Agriculture Forest Service Federal Pathway Program during his time at SUNY-ESF. The support of the New York State Energy Research and Development Authority (NYSERDA) in providing funds for the monitoring at the Arbutus Watershed and Huntington Forest is also greatly appreciated. The authors would also like to thank Pat McHale, Joshua Gomez, Cheryl Glor, and the staff of the Adirondack Ecological Center in Newcomb, NY, for their help in the field and laboratory.

References

Beaulieu, J. J., Arango, C. P., Hamilton, S. K., & Tank, J. L. (2008). The production and emission of nitrous oxide from headwater streams in the Midwestern United States. *Global Change Biology, 14*(4), 878–894.

Beaulieu, J. J., Tank, J. L., Hamilton, S. K., Wollheim, W. M., Hall, R. O., Mulholland, P. J., Peterson, B. J., Ashkenas, L. R., Cooper, L. W., Dahm, C. M., Dodds, W. K., Grimm, N. B., Johnson, S. L., McDowell, W. H., Poole, G. C., Valett, H. M., Arango, C. P., Bernot, M. J., Burgin, A. J., Crenshaw, C. L., Helton, H. M., Johnson, L. T., O'Brien, J. M., Potter, J. D., Sheibley, R. W., Sobota, D. J., & Thomas, S. M. (2011). Nitrous oxide emission from denitrification in stream and river networks. *PNAS, 108*(1), 214–219. doi:10.1073/pnas.1011464108.

Billett, M. F., & Moore, T. R. (2008). Supersaturation and evasion of CO_2 and CH_4 in surface waters at Mer Bleue peatland. *Canada Hydrology Process, 22*(12), 2044–2054.

Bowden, W. B., & Bormann, F. H. (1986). Transport and loss of nitrous oxide in soil water after forest clear-cutting. *Science, 233*(4766), 867.

Burgin, A.J., & Groffman, P.M. (2012). Soil O_2 controls denitrification rates and N_2O yield in a riparian wetland. *Journal of Geophysical Research: Biogeosciences*, (2005–2012), 117(G1).

Butman, D., & Raymond, P. (2011). Significant efflux of carbon dioxide from streams and rivers in the United States. *Nature Geoscience*. doi:10.1038/NGEO1294.

Butman, D., Stackpoole, S., Stets, E., McDonald, C. P., Clow, D. W., & Striegl, R. G. (2016). Aquatic carbon cycling in the conterminous United States and implications for terrestrial carbon accounting. *PNAS, 113*(1), 58–63. doi:10.1073/pnas.1512651112.

Christopher, S. F., Page, B. D., Campbell, J. L., & Mitchell, M. J. (2006). Contrasting stream water NO_3^- and Ca_2^+ in two nearly adjacent catchments: the role of soil Ca and forest vegetation. *Global Change Biology, 12*(2), 364–381.

Clesceri, L. S., Greenberg, A. E., & Eaton, A. D. (1998). *Standard methods for the examination of water and waste water*. Washington: American Public Health Association.

Clymo, R. S., Pearce, D. M., & Conrad, R. (1995). Methane and carbon dioxide production in, transport through, and efflux from a peatland [and discussion]. *Philosophical Transactions of the Royal Society of London Series A: Physical and Engineering Sciences, 351*(1696), 249–259.

Dent, C. L., Grimm, N. B., & Fisher, S. G. (2001). Multiscale effects of surface–subsurface exchange on stream water nutrient concentrations. *Journal of the North American Benthological Society, 20*(2), 162–181.

Fisher, K., Jacinthe, P. A., Vidon, P., Liu, X., & Baker, M. E. (2014). Nitrous oxide emission from cropland and adjacent riparian buffers in contrasting hydrogeomorphic settings. *Journal of Environmental Quality, 43*(1), 338–348. doi:10.2134/jeq2013.06.0223.

Gomez, J., Vidon, P., Gross, J., Beier, C., Caputo, J., & Mitchell, M. (2016). Estimating greenhouse gas emissions at the soil-atmosphere interface in forested watersheds of the US Northeast. *Environmental Monitoring and Assessment, 188*(295), 1–16. doi:10.1007/s10661-016-5297-0.

Hedin, L. O., von Fischer, J. C., Ostrom, N. E., Kennedy, B. P., Brown, M. G., & Robertson, G. P. (1998). Thermodynamic constraints on nitrogen transformations and other biogeochemical processes at soil-stream interfaces. *Ecology, 79*(2), 684–703.

Hefting, M. M., Bobbink, R., & de Caluwe, H. (2003). Nitrous oxide emission and denitrification in chronically nitrate-loaded riparian buffer zones. *Journal of Environmental Quality, 32*(4), 1194–1203.

Hope, D., Palmer, S., Billett, M. F., & Dawson, J. J. (2001). Carbon dioxide and methane evasion from a temperate peatland stream. *Limnology Oceanography, 46*(4), 847–857.

Jacinthe, P. A., & Groffman, P. M. (2001). Silicone rubber sampler to measure dissolved gases in saturated soils and waters. *Soil Biology and Biochemistry, 33*(7), 907–912.

Jacinthe, P. A., & Lal, R. (2004). Effects of soil cover and land-use on the relations flux-concentration of trace gases. *Soil Science, 169*(4), 243–259.

Jacinthe, P. A., Bills, J. S., Tedesco, L. P., & Barr, R. C. (2012). Nitrous oxide emission from riparian buffers in relation to vegetation and flood frequency. *Journal of Environmental Quality*. doi:10.2134/jeq2011.0308.

Kasahara, T., & Hill, A. R. (2005). Effects of riffle-step restoration on hyporheic zone chemistry in N-rich lowland streams. *Canadian Journal of Fisheries and Aquatic Sciences, 63*, 120–133.

McClain, M. E., Boyer, E. W., Dent, C. L., Gergel, S. E., Grimm, N. B., Groffman, P. M., Hart, S. C., Harvey, J. W., Johnston, C. A., Mayorga, E., McDowell, W. H., & Pinay, G. (2003). Biogeochemical hotspots and hot moments at the interface of terrestrial and aquatic ecosystems. *Ecosystems, 6*, 301–312.

Mitchell, M. J., Raynal, D. J., & Driscoll, C. T. (2009). *Response of Adirondack ecosystems to atmospheric pollutants and climate change at the Huntington forest and arbutus watershed: research findings and implications for public policy. Synthesis report*. Albany: New York State Energy Research and Development Authority (NYSERDA).

Morse, J. L., Ardón, M., & Bernhardt, E. S. (2012). Greenhouse gas fluxes in southeastern US coastal plain wetlands under contrasting land uses. *Ecological Application, 22*(1), 264–280.

Mosier, A., Kroeze, C., Nevison, C., Oenema, O., Seitzinger, S., & Van Cleemput, O. (1998). Closing the global N2O budget: nitrous oxide emissions through the agricultural nitrogen cycle. *Nutrient Cycling in Agroecosystems, 52*(2–3), 225–248.

Naiman, R. J., Decamps, H., & McClain, M. E. (2010). *Riparia: ecology, conservation, and management of streamside communities*. London: Academic Press, Elsevier. 430 pages.

Raymond, P. A., Hartmann, J., Lauerwald, R., Sobek, S., McDonald, C., Hoover, M., Butman, D., Striegl, R. G., Mayorga, E., Humborg, C., Kortelainen, P., Durr, H., Meybeck, M., Ciais, P., & Guth, P. (2013). Global carbon dioxide emissions from inland waters. *Nature, 503*, 355–359. doi:10.1038/nature12760.

Rosamond, M. S., Thuss, S. J., & Schiff, S. L. (2012). Dependence of riverine nitrous oxide emissions on dissolved oxygen levels. *Nature Geoscience, 5*, 715–718.

Rothfuss, F., & Conrad, R. (1998). Effect of gas bubbles on the diffusive flux of methane in anoxic paddy soil. *Limnology and Oceanography, 43*(7), 1511–1518.

Sanders, I. A., Heppell, C. M., Cotton, J. A., Wharton, G., Hildrew, A. G., Flowers, E. J., & Trimmer, M. (2007). Emission of methane from chalk streams has potential implications for agricultural practices. *Freshwater Biology, 52*(6), 1176–1186.

Somers, R. C. (1986). *Soil classification, genesis, morphology and variability of soils found within the central Adirondack region of New York, State University of New York*. Syracuse: College of Environmental Science and Forestry. http://www.esf.edu/aec/publications/.

Stanley, E. H., Casson, N. J., Christel, S. T., Crawford, J. T., Loken, L. C., & Oliver, S. K. (2016). The ecology of methane in streams and rivers: patterns, controls, and global significance. *Ecological Monographs, 86*, 146–171. doi:10.1890/15-1027.

Ullah, S., & Moore, T.R. (2011). Biogeochemical controls on methane, nitrous oxide, and carbon dioxide fluxes from deciduous forest soils in eastern Canada. *Journal of Geophysical Research: Biogeosciences*, (2005–2012), 116(G3).

van Hulzen, J. B., Segers, R., van Bodegom, P. M., & Leffelaar, P. A. (1999). Temperature effects on soil methane production: an explanation for observed variability. *Soil Biology and Biochemistry, 31*, 1919–1929. doi:10.1016/S0038-0717(99)00109-1.

Vidon, P., & Hill, A. R. (2004). Denitrification and patterns of electron donors and acceptors in eight riparian zones with contrasting hydrogeology. *Biogeochemistry, 71*, 259–283. doi:10.1007/s10533-004-9684-1.

Vidon, P., Allan, C., Burns, D., Duval, T. P., Gurwick, N., Inamdar, S., Lowrance, R., Okay, J., Scott, D., & Sebestyen, S. (2010). Hot spots and hot moments in riparian zones: potential for improved water quality management. *Journal of the American Water Resources Association, 46*(2), 278–298.

Werner, S. F., Browne, B. A., & Driscoll, C. T. (2012). Three-dimensional spatial patterns of trace gas concentrations in baseflow-dominated agricultural streams: implications for surface-ground water interactions and biogeochemistry. *Biogeochemistry, 107*, 319–338.